Science of the Total Environment 697 (2019) 134119

Contents lists available at ScienceDirect

Science of the Total Environment

journal homepage: www.elsevier.com/locate/scitotenv

Enhanced removal of hexavalent chromium by engineered biochar composite fabricated from phosphogypsum and distillers grains

Guoqi Lian [a,c,d], Bing Wang [a,b,c,*], Xinqing Lee [c], Ling Li [c], Taoze Liu [e], Wenqiang Lyu [f]

[a] College of Resource and Environmental Engineering, Guizhou University, Guiyang 550025, Guizhou, China
[b] Key Laboratory of Karst Environment and Geohazard, Ministry of Natural Resources, Guiyang 550025, Guizhou, China
[c] State Key Laboratory of Environmental Geochemistry, Institute of Geochemistry, Chinese Academy of Sciences, Guiyang 550081, China
[d] University of Chinese Academy of Sciences, Beijing 100049, China
[e] College of Eco-Environmental Engineering, Guizhou Minzu University, Guiyang 550025, China
[f] Institute of Guizhou Mountain Resources, Guizhou Academy of Sciences, Guiyang 550001, China

HIGHLIGHTS

- A novel biochar composite was synthesized from distillers grains and phosphogypsum for Cr(VI) removal.
- Batch adsorption experiments were conducted on the adsorption characteristics of Cr(VI).
- The maximum Cr(VI)adsorption capacity reached 157.9 mg g^{-1}.
- The composites can be used as a high-quality and low-cost adsorbent for Cr (VI) removal.

GRAPHICAL ABSTRACT

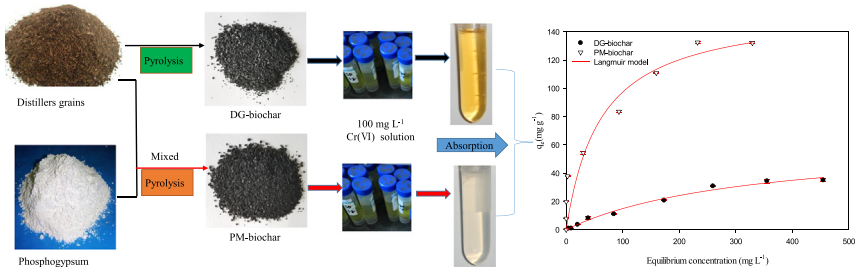

ARTICLE INFO

Article history:
Received 18 June 2019
Received in revised form 30 July 2019
Accepted 25 August 2019
Available online 29 August 2019

Editor: Filip M.G. Tack

Keywords:
Distillers grains
Phosphogypsum
Pyrolysis temperature
Hexavalent chromium
Adsorption

ABSTRACT

Two kinds of industrial wastes (distillers grains and phosphogypsum) were used as raw materials to produce a new biochar composite for Cr(VI) removal in water. The influencing factors including pyrolysis temperature, dosage, initial solution pH as well as contacting time were explored. The adsorption kinetics, isotherms, and thermodynamics of two biochars were conducted. The results show that the adsorption of Cr(VI) by biochar is related to pH. The ideal pH was 3.0 and the adsorbed Cr(VI) decreases as the pH increases. The Cr(VI) adsorption process conformed to the pseudo-second-order equation. Phosphogypsum modified (PM)-biochar is well described by the Freundlich model. The maximum adsorption capacities of distillers grains (DG)-biochar and PM-biochar on Cr(VI) were 63.1 and 157.9 mg g^{-1}, respectively. The thermodynamic analysis indicates that the Cr(VI) adsorption occurs spontaneously which is an endothermic process. This study provided an alternative way for Cr(VI) removal from water.

© 2019 Elsevier B.V. All rights reserved.

1. Introduction

Heavy metals are critical contaminants in industrial wastewater, which are potentially harmful to human health and ecological environment (Pratush et al., 2018). Among them, chromium (Cr) is one of the most harmful elements. Cr and its compounds are widely found in metallurgical, chemical, mineral engineering, leather tanning, textile

* Corresponding author at: College of Resource and Environmental Engineering, Guizhou University, Guiyang 550025, Guizhou, China.
E-mail address: wangbing@vip.gyig.ac.cn (B. Wang).

https://doi.org/10.1016/j.scitotenv.2019.134119
0048-9697/© 2019 Elsevier B.V. All rights reserved.

Table 1
The physicochemical properties of the biochar.

Adsorbent	Yield	pH	pH of zero charge	EC μs cm^{-1}	Elemental contents						Ash %	Volatile %
					C wt%	H wt%	N wt%	S wt%	H/C_{tot} mol mol^{-1}	C/N ratio		
DG-biochar	29.8%	9.02	3.06	395	66.71	2.40	5.27	0.30	0.43	12.67	28.15	46.56
PM-biochar	36.9%	10.10	7.74	2950	40.22	1.54	2.97	5.62	0.72	13.56	36.51	50.44

dyeing, metal plating, and other production industries. Cr is considered to be a major contaminant causing serious environmental and public health problems (Kim et al., 2002). The above-mentioned production process produces a large amount of chromium-containing wastewater. The soil, groundwater, and surface water caused by chromium pollution seriously threaten the ecological environment and human health. The allowable concentration of Cr(VI) in the surface water of theWHO is 0.1 mg L^{-1}, which is 0.05 mg L^{-1} in drinking water (EPA, 1990; Sahu et al., 2009). The industries enterprises have to cut downthe Cr(VI) concentration to allowable valuebefore it is discharged, otherwise, it will incur significant treatment costs (Baral and Engelken, 2002). Chromium cannot be degraded by microorganisms in water, and can only be transformed, dispersed and enriched in different species. The toxicity of each chromium compound is different. In a water environment, the main valence of chromium in the compounds is trivalent and hexavalent, and Cr (VI) is regarded as the most toxic. It is easily enriched by the food chain and is difficult to degrade. It can also break into the human body via the skin, digestive tract, and mucous membranes, thus affecting human health (Pellerin and Booker, 2000; Zhao et al., 2014). Therefore, the removal of Cr(VI) from wastewater through scientific and effective technology before discharge is essential to ensure water quality and human health.

At present, many strategies have been proposed for elimination Cr(VI) from wastewater containing Cr(VI) (Chen et al., 2009; Gheju and Balcu, 2011; Kumar et al., 2008; Kurniawan et al., 2006; Mao et al., 2012; Namasivayam and Sureshkumar, 2008; Owlad et al., 2009; Saha and Orvig, 2010; Zhou and Chen, 2010). Different methods have their own pros and cons, and there are certain scopes and limitations. The sludge produced by the chemical precipitation method has a relatively large water content, which causes difficulty in dehydration, increases operating costs, and is liable to cause secondary pollution. The ion exchange method is difficult to promote due to a series of problems such as easy poisoning of the resin, low exchange capacity, poor selectivity, and regeneration ability, short service life, and generation of more waste liquid. Compared with other technologies, the adsorption has been extensively applied for the treatment of wastewater due to its high efficiency, cost-effective and easy to use and recycle Cr. Currently, a variety of adsorbents have been adopted to remove Cr(VI) from water (Dehghani et al., 2016; Hu et al., 2005; Lim and Aris, 2014; Zhao et al., 2018). However, because physicochemical properties of different adsorbent materials vary greatly, the removal of Cr(VI) in water still faces some problems (Aksu et al., 2002). Commonly used adsorbents are mainly activated carbon, bentonite, diatomaceous earth, zeolite, humus

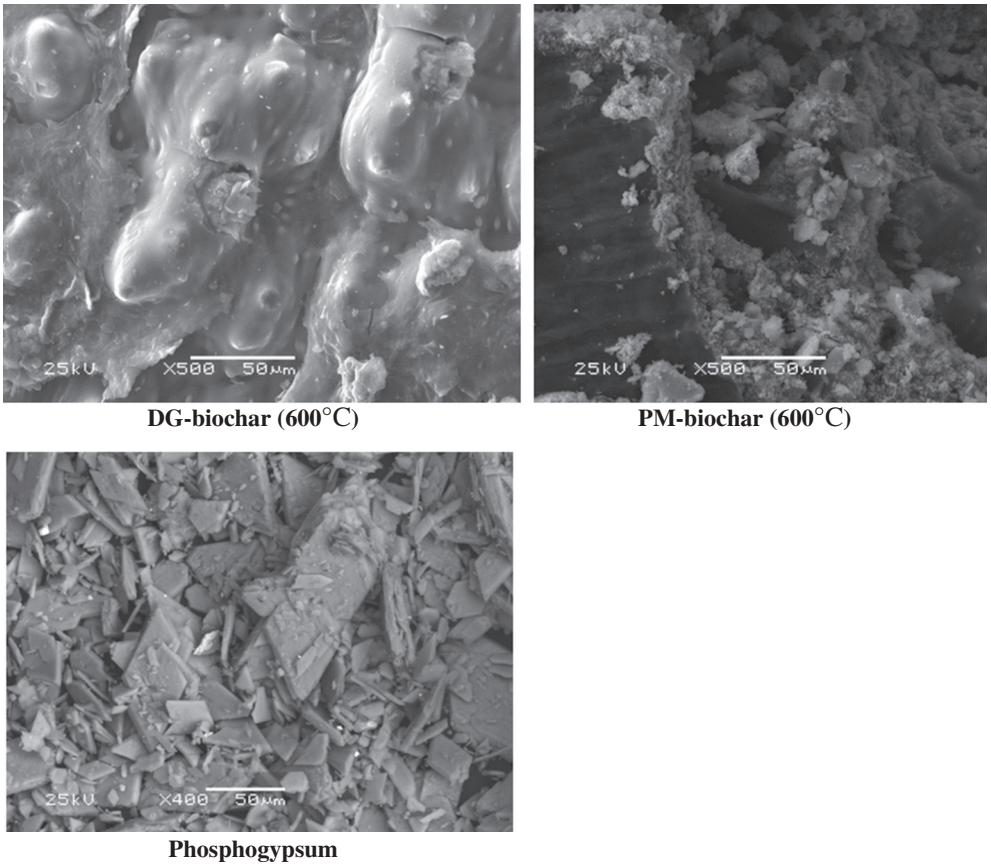

Fig. 1. SEM images of different biochars and phosphogypsum.

resin and so on. Although the above adsorbents have excellent performance, there are still some disadvantages such as the high price of adsorbent materials, single adsorption type. Therefore, it is urgent to find a high efficiency and low-cost Cr(VI) treatment method.

Biochar is widely used for remediation of contaminants in the environment (Ahmad et al., 2014; Mohan et al., 2014; Shaheen et al., 2019; B. Wang et al., 2018; Q. Wang et al., 2018; Xiao et al., 2018). However, the newly prepared biochar, which is often negatively charged, can only adsorb most of the cations. Most of the biochar has no adsorption to anions or limited adsorption capacity. Therefore, it is essential to optimize the newly prepared biochar to improve its adsorption capacity for anions. Different methods have been used to modify biochar to expand its range of applications in environmental remediation to meet different needs (Dong et al., 2017; Han et al., 2016; Miretzky and Cirelli, 2010; Rajapaksha et al., 2016; Shi et al., 2018; Wang et al., 2017, 2019; Yu et al., 2018; Zhao et al., 2017). Although the adsorption performance of engineered biochar has been improved through modification, the production cost of most modified biochar is relatively high, which inhibits its large-scale promotion and popularization. Therefore, it is particularly important to enhance its adsorption performance for anions and reduce its production cost.

As a by-product of brewing enterprises, distillers grains have high water content and high acidity (Liu and Rosentrater, 2016). Therefore, if they are not treated properly, they will be easily spoiled and deteriorated. This will not only waste precious resources but also cause serious pollution to the surrounding environment. As an industrial by-product of anaerobic fermentation, distillers grains could be an excellent feedstock for the production of biochar. Meanwhile, phosphogypsum is a solid waste residue produced by treating phosphate rock with sulfuric acid in the production of phosphoric acid, and its main component is calcium sulfate. Phosphogypsum not only occupies a large amount of land but also seriously pollutes the environment (Rutherford et al., 1994). Therefore, how to use it properly for resource utilization has become an urgent problem to be solved.

The primary purposes of this study include (i) synthesize a novel of biochar composite using distillers grains and phosphogypsum as raw materials, (ii) investigate the influence of pyrolysis temperature, dosage, solution pH and other factors on the Cr(VI) adsorption behavior, so as to screen out the optimal pyrolysis and adsorption conditions, and (iii) figure out the adsorption behavior and mechanism through batch adsorption experiments on the adsorption kinetics, isotherms, and thermodynamics of Cr(VI) in water.

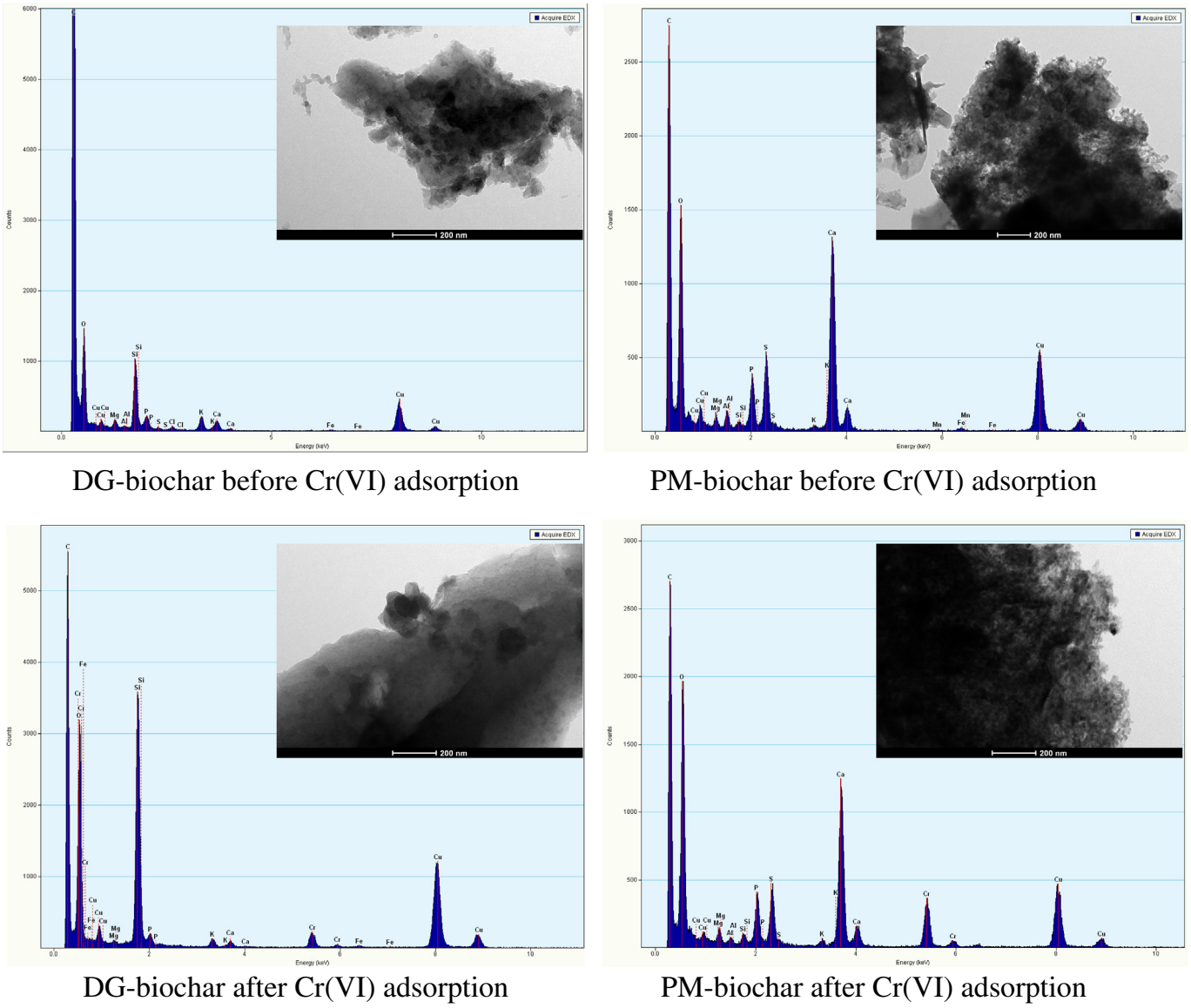

Fig. 2. TEM images of DG-biochar and PM-biochar before and after Cr(VI) adsorption.

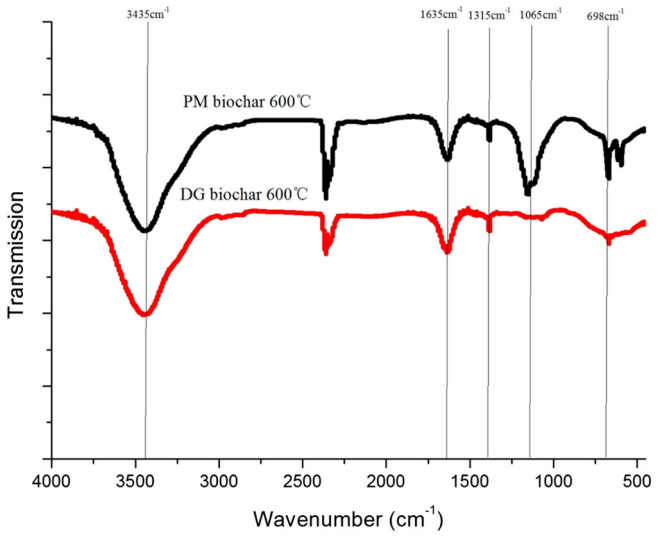

Fig. 3. FTIR spectra of DG-biochar and PM-biochar.

2. Material and methods

2.1. Chemicals and reagents

Reagents used in the experiment include potassium dichromate ($K_2Cr_2O_7$), sulfuric acid (H_2SO_4), sodium hydroxide (NaOH), phosphate acid (H_3PO_4), acetone and diphenylcarbazide. All glassware and PE centrifuge tubes are washed with acid (10% hydrochloric acid) and washed with DI water.

2.2. Preparation of biochar

Distillers grains were collected from a local distillery, Guizhou province, China. Phosphogypsum was collected from a phosphate fertilizer plant, Guizhou province, China. The distillers grains and phosphogypsum were dried at 105 °C in the oven. The phosphogypsum was mixed with the distillers grains in a ratio of 1:2, and then the mixture was thoroughly stirred by adding an appropriate amount of DI water and dried at 105 °C and then sealed and stored for subsequent pyrolysis. Biochar was prepared from distillers grains and phosphogypsum mixture in a Tubular carbonization furnace. The treated raw materials are pyrolyzed at three temperatures from 300 °C to 600 °C. In order to get the best pyrolysis condition, biochar prepared at different pyrolysis

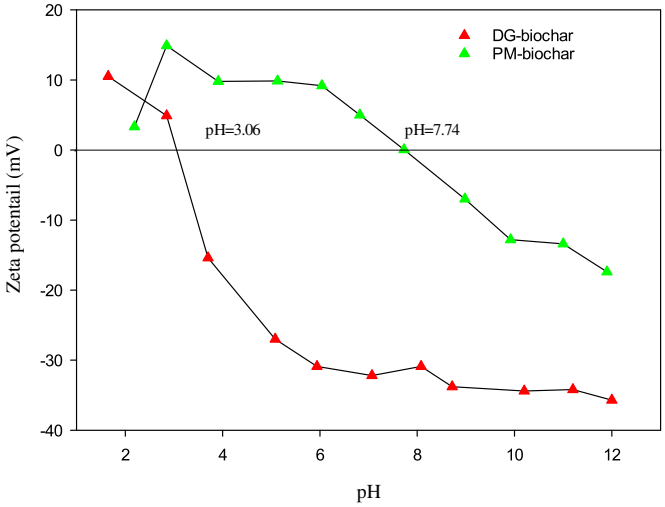

Fig. 4. The relationship between pH and Zeta potential.

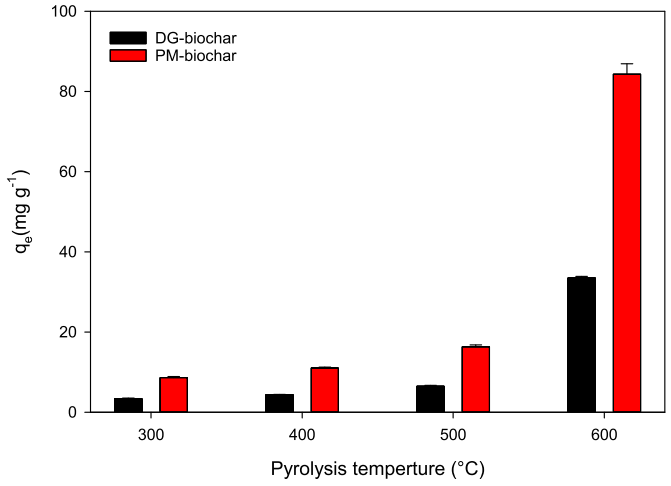

Fig. 5. Adsorption of Cr(VI) by biochar pyrolysis at different temperatures.

temperatures which are labeled as: Distillers grains (DG)-biochar (300 °C), DG-biochar (400 °C), DG-biochar (500 °C), DG-biochar (600 °C), phosphogypsum modified (PM)-biochar (300 °C), PM-biochar (400 °C), PM-biochar (500 °C), PM-biochar (600 °C).

2.3. Biochar characterization

Surface morphology, surface functional groups, proximate analysis and elemental analysis of biochars was analyzed according to the classic methods (ASTM, 2007; Wang et al., 2015). The BET methodology was adopted in the measurement of the SSA of the sorbent with N_2 adsorption. The pH value of biochar samples was determined by combining biochar with water at a mass ratio of 1:20 with a pH meter. The surface zeta potential of the biochars was measured by a Malvern Zeta meter (Nano ZSE + MPT2, Malvern Panalytical Instruments Ltd., UK).

2.4. Adsorption experiments

50 mL PE centrifugal tubes were used to conduct all the adsorption experiment at room temperature (22 ± 0.5 °C). A stock solution of Cr (VI) is dissolved by the optimal pure $K_2Cr_2O_7$ in ultrapure water. All samples were shaken at 300 rpm with triplicate for 24 h. A diphenylcarbazide method was used to analyze the concentration of Cr(VI) and the absorbance of 540 nm was determined by UV–vis spectrophotometer (Model 721, Shanghai Metash Instruments Co., Ltd., China) (Pan et al., 2014; Park et al., 2008).

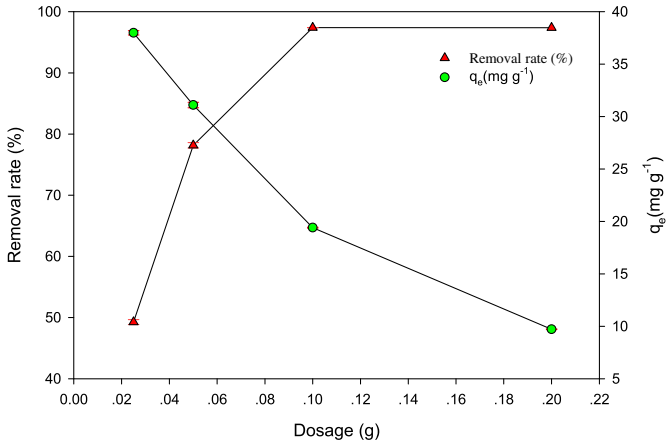

Fig. 6. The relationship between dosage and Cr(VI) adsorption capacity.

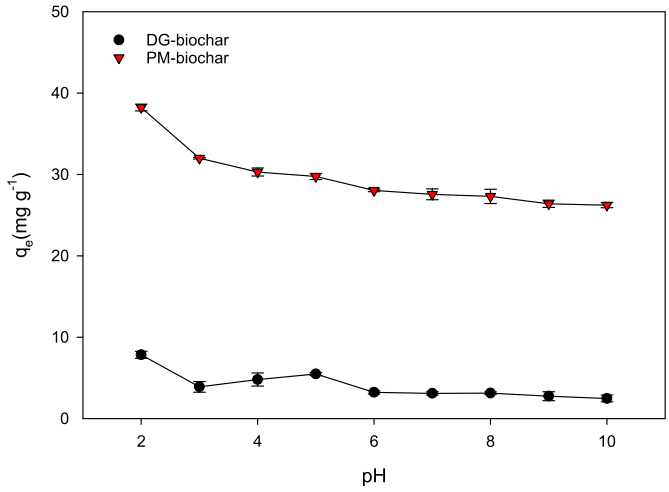

Fig. 7. Effect of pH on Cr(VI) adsorption at 25 °C, adsorbent dose, 50 mg L^{-1} of $K_2Cr_2O_7$solution.

For the purpose of getting the optimum dosage, the adsorption experiment was conducted with a range of dosage of 0.0250 g, 0.0500 g, 0.1000 g, and 0.2000 g. The procedures are the same as described above. The Cr(VI) content was determined immediately after filtration.

Both the initial pH of solution and the background electrolyte have an effect on the heavy metals adsorption performance (Jiang et al., 2017; Tong et al., 2011; Zhou et al., 2017). In this study, the effect of pH on Cr(VI) adsorption were conducted by adjusting the initial pH of 100 mg·L^{-1} Cr(VI) solutions to 3.0, 4.0, 5.0, 6.0, 7.0, 8.0, 9.0, 10.0, 11.0 and 12.0 using 0.1 M H_2SO_4 and 0.1 M NaOH solution. 0.0500 g of biochar was added into 40 mL of the above different pH Cr(VI) solution, shaken at 300 rpm for 24 h, and the Cr(VI) content was measured after filtration.

Sorption kinetics of Cr(VI) was examined using100 mg·L^{-1} Cr(VI) standard solution with a pH of 3.0 at time interval of 0.083, 0.25, 0.5, 1, 2, 4, 8, 16, and 24 h, respectively. Sorption isotherms were carried out by varying concentrations (5, 10, 25, 50, 100, 200, 300, 400, 500 mg L^{-1}) with a pH of 3.0 shaken for 24 h. The supernatant was taken for measuring the concentration of Cr(VI). Adsorption thermodynamics were conducted in the environment of 16 °C, 26 °C, 36 °C, respectively. After shaking for 24 h, the supernatant was taken for Cr (VI) determination.

Table 2
Summary best-fit parameters of various kinetic models for Cr(VI) adsorption onto biochar.

Adsorbent	Model	Parameter 1	Parameter 2	R^2
DG-biochar	Pseudo-first-order	$k_1 = 1.888$	$q_e = 6.3$	0.875
	Pseudo-second-order	$k_2 = 0.3981$	$q_e = 6.7$	0.947
	Elovich	$\alpha = 96.119$	$\beta = 1.055$	0.999
	Ritchie	$k_n = 0.00026$	$q_e = 6.26$	0.768
PM-biochar	Pseudo-first-order	$k_1 = 1.739$	$q_e = 33.2$	0.95
	Pseudo-second-order	$k_2 = 0.0667$	$q_e = 35.7$	0.983
	Elovich	$\alpha = 360.97$	$\beta = 0.190$	0.975
	Ritchie	$k_n = 0.000193$	$q_e = 33.1$	0.916

3. Results and discussion

3.1. Characterization of the samples

The physicochemical properties of the biochar are listed in Table 1. Surface morphologies of the DG-biochar and PM-biochars are shown in Fig. 1. These SEM images clearly describe the surface morphological characteristics of the two materials. It can be seen that the surface of the DG-biochar is smooth after pyrolysis and has a large number of pore structures. After pyrolysis with phosphogypsum, the surface of the PM-biochar forms a distinct pore structure and becomes rough due to the adhesion of calcium oxides. Moreover, flocculent particles are also formed on the surface of PM-biochar. Compared with the DG-biochar, the PM-biochar has a higher H/C value, indicating that its structure contains abundant oxygen-containing functional groups. Combined with the TEM-EDS results (Fig. 2), it can be found from the TEM-EDS spectrum that DG-biochar is mainly composed of carbon, oxygen, and silicon, and PM-biochar has a lot of calcium added to its surface after being modified with phosphogypsum. The TEM-EDS pattern of the adsorbed biochar surface suggests that Cr(VI) adsorption on the biochar could be through surface precipitation and electrostatic adsorption (Dong et al., 2017).

Fig. 3 shows the infrared spectrum of the biochar and PM-biochar. In the infrared spectrum of PM-biochar, we can clearly see that there are distinct absorption peaks between the wavenumbers of 1635, 1065 and 698 cm^{-1}. Among them, the characteristic peak with an absorption peak of 1635 cm^{-1} may be the carbonyl group of the carboxyl group in biochar. The peak with a wavenumber of 1065 cm^{-1} may be a C—O functional group. The characteristic peak of 698 cm^{-1} is generated by Ca—O stretching vibration, which indicates that Ca is successfully embedded in the biochar.

The SSA, pore volume, as well as pore size of the DG-biochar and PM-biochar, differed. Among them, the BET SSA (13.67 m^2 g^{-1}) of PM-

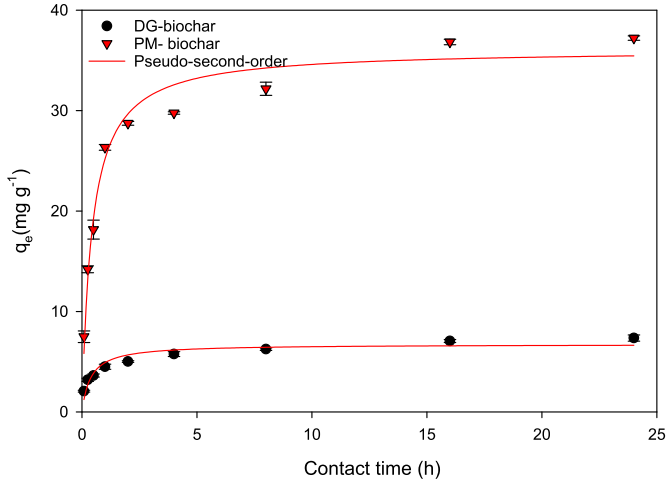

Fig. 8. The relationship between the amount of adsorption and the proper time.

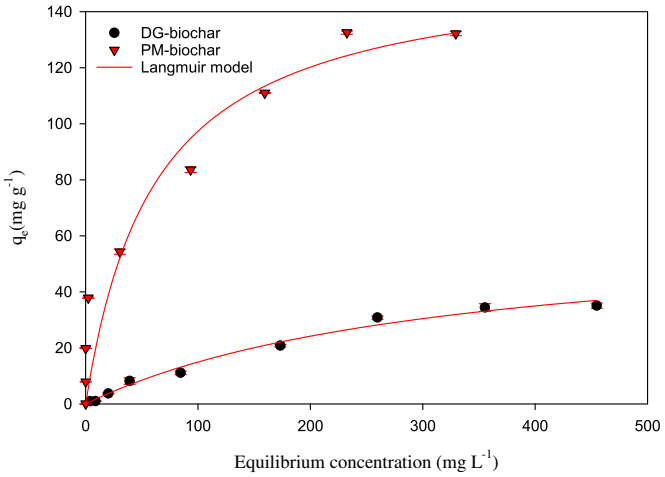

Fig. 9. Equilibrium concentration and adsorption.

Table 3
Summary best-fit isotherm model parameters for sorption of Cr(VI) onto the sorbents.

Adsorbent	Langmuir adsorption model			Freundlich adsorption model		
	Q_0 (mg g^{-1})	k_L	R^2	k_f	1/n	R^2
DG-biochar	63.1	0.003	0.987	0.71	1.53	0.978
PM-biochar	157.9	0.016	0.923	21.35	3.13	0.975

biochar is larger than the BET SSA (0.92 m^2 g^{-1}) of DG-biochar. The pore volume of the PM-biochar (0.0096 m^3 g^{-1}) is larger than the pore volume of the distillers grain biochar (0.0005 m^3 g^{-1}), indicating that the SSA and pore structure of the distillers grain biochar is changed by pyrolysis with phosphogypsum.

According to the result of zeta potential, the zeta potential of the DG-biochar is −36.6 mV, and the zeta potential of the PM-biochar is 0.949 mV. The zeta potential of PM-biochar is higher than DG-biochar. Protonation may occur on the PM-biochar surface which creates a partial positive charge helping phosphate sorption via electrostatic attraction. As shown in Fig. 4, the pH_{pzc} of DG-biochar is 3.06 and that of PM-biochar is 7.74. When the solution pH > pH_{pzc}, the surface of the adsorbent undergoes a deprotonation reaction, which is favorable for cations adsorption; when the solution pH < pH_{pzc}, protonation occurs on the surface of the biochar, giving the adsorbent surface a positive charge, which is beneficial to anions adsorption.

3.2. Effect of pyrolysis temperature

The generation of surface functional groups of biochar is directly affected by pyrolysis temperature during the preparation of biochar, thereby affecting the ability of biochar to remove contaminants (Han et al., 2016; Wang et al., 2016). As shown in Fig. 5, with the pyrolysis temperature increases, the adsorbed Cr(VI) amount by both biochars increases. It indicates that the high temperature helps to attach more calcium to the surface of the biochar during the pyrolysis process, thereby contributing to the Cr(VI) adsorption. In addition, as the pyrolysis temperature increases, the pore structure and SSA of the biochar increase accordingly, which is favorable to the Cr(VI) adsorption.

3.3. Effect of dosage

The adsorption amount and removal rate of Cr(VI) by biochar is shown in Fig. 6. With the increase of biochar dosage, the adsorption amount increased gradually and then decreased. When the dosage was 500 mg, the maximum adsorption amount was reached. The removal rate of Cr(VI) by biochar gradually increases with the increase of adsorbent dosage, and then rises sharply and then slows down. Considering the aspects of both efficiency and cost, the optimum dosage is 500 mg.

3.4. Effect of solution pH

The initial pH of solution strongly influences the surface charge, ionization of the adsorbed species, and the type of ions, thereby affecting the Cr(VI) adsorption process. The effect of solution pH on the removal of Cr(VI) ions is primarily to influence the presence of Cr(VI) and the surface charge (Rajapaksha et al., 2018; Zhou et al., 2011). Cr(VI) mostly exists in the form of $Cr_2O_7^{2-}$ and $HCrO_4^-$ when the pH of the solution is low, which can be combined with the active site of protonation by electrostatic adsorption. The surface of biochar is forced to be positively charged under low pH condition, causing it easy to adsorb negatively charged $HCrO_4^-$ and $Cr_2O_7^{2-}$. There are more H^+ on the surface of biochar at a lower value, which leads to more positive charge enhancing the attraction between the adsorption site and Cr(VI). As shown in Fig. 7, the maximum adsorbed amount of Cr(VI) is reached at pH = 2.0. A large amount of H^+ and $Cr_2O_7^{2-}$ are existed under acidic conditions (pH = 2–3), and the number of protons participating in the reaction is large. This protonation effect promotes the electrostatic adsorption of the adsorbent to Cr(VI) ions. As the pH increases, Cr(VI) gradually The CrO_4^{2-} form exists, and it will compete with CrO_4^{2-} due to the increase of OH^- concentration. At the same time, the surface of biochar is gradually negatively charged. The repulsive force between Cr(VI) and OH^- increases, which is not conducive to adsorption. At a pH of 3.0–6.0, Cr(VI) in the solution is mainly presented as $HCrO_4^-$ and $Cr_2O_7^{2-}$, and when the pH is higher than 7.0, Cr(VI) is mostly presented as CrO_4^{2-}. As the pH of the solution increases, the adsorption capacity of biochar to Cr(VI) ions gradually decreases (López-García et al., 2010). When pH >7.0, the Cr(VI) adsorption capacity of biochar is significantly decreased because the affinity of biochar oxygen groups to OH^- is greater than that of $Cr_2O_7^{2-}$. As the pH of Cr(VI) solution increases, OH^- increases and CrO_4^{2-} negative ions are dominant in solution, and the ionic radius becomes large, which causes these adsorbents to repel CrO_4^{2-}, and the adsorption efficiency is lowered. Considering the pH of actual wastewater, this study chose to set the pH of the solution to 3.0 for subsequent studies.

3.5. Adsorption kinetics

The results of the adsorption kinetics are shown in Fig. 8. The adsorption rate of Cr(VI) is fast in the initial stage (4 h). After 4 h, the adsorption rate decreases, and finally reaches the adsorption equilibrium. This is attributed to sufficient active adsorption sites, pore structure and surface functional groups on the surface of the biochar at the initial adsorption stage. As the adsorption process proceeds, the active site of the adsorbent is occupied by the Cr(VI) ions in the solution which results

Table 4
Previously reported adsorption capacities of Cr(VI) onto various biochar.

Adsorbent	Temperature (°C)	Q_0 (mg g^{-1})	pH	Ref
Porous zinc-biochar nanocomposites	450	102.66	2.0	(Gan et al., 2015)
β-Cyclodextrin–chitosan modified biochars	450	206	2.0	(Huang et al., 2016)
Corn-bran residue and derived chars	–	86.49	2.0	(Zhang and Zheng, 2015)
Magnetic biochar	700	42.7	–	(Yang et al., 2017)
Magnetic biochar	650	61.97	–	(Ouyang et al., 2017)
Walnut shells biochar	450	36.55	2.0	(Altun and Kar, 2016)
Walnut shells biochar	450	49.76	2.0	(Altun and Kar, 2016)
H_3PO_4-activated cattail carbon	469.02	59.54	2.2	(Shu et al., 2018)
Sugar beet tailing biochar	300	123	2.0	(Dong et al., 2011)
$ZnCl_2$ activated carbon	400	90.90	2.0	(Rangabhashiyam and Selvaraju, 2015)
Raw Sterculia guttata shell biochar	400	12.46	2.0	
Graphene oxide coated water hyacinth biochar composite	300	150.02	2.0	(Shang et al., 2016)
Biochar from sugar beet tailing	300	123	2.0	(Dong et al., 2011)
DG-biochar	600	63.1	3.0	This study
PM-biochar	600	157.9	3.0	This study

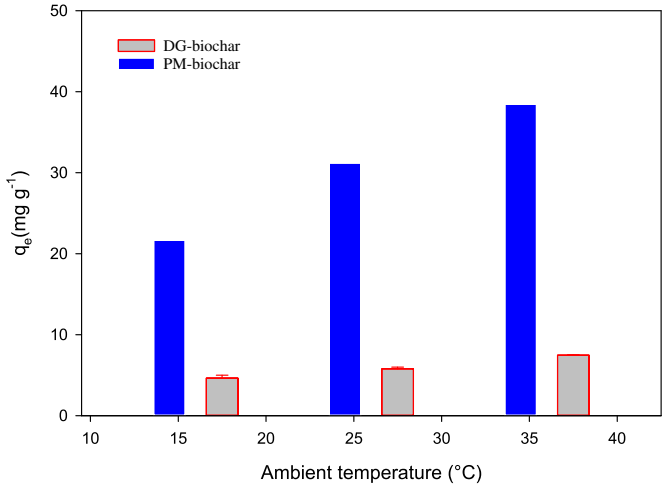

Fig. 10. The relationship between adsorption and ambient temperature.

in the pore structure to be filled. Meanwhile, the number of functional groups decreased, and the charge after adsorption of Cr(VI) was gradually the same as the charge on the Cr(VI) in the solution, which produced a repulsive force, making the adsorption reaction difficult. Furthermore, Cr(VI) in the solution undergoes a complexation reaction with the functional groups of adsorbent and is stabilized on the biochar in the form of a complex. The above factors lead to the reduction of Cr (VI) concentration gradient, so the adsorption rate is gradually lowered. The time required to reach the adsorption equilibrium is about 24 h. After 24 h, the amount of adsorption did not change much, and the adsorption was basically completed and tends to be balanced. It is considered that the adsorption equilibrium has been reached after adsorption for 24 h in the subsequent adsorption experiment. At this time, the adsorption amount reaches 32.0 mg g^{-1}.

To further figure out the adsorption mechanism, the data of adsorption kinetics were simulated by the mathematical model. Pseudo-first-order, pseudo-second-order models, Elovich model, and Ritchie model are tested with the following equations.

$$q_t = q_e\left(1-e^{-kt}\right) \quad \text{Pseudo-first-order model} \tag{1}$$

$$q_t = \frac{kq_e{}^2 t}{1+kq_e t} \quad \text{Pseudo-second-order model} \tag{2}$$

$$q_t = \frac{1}{\beta}\ln(\beta\alpha t+1) \quad \text{Elovich model} \tag{3}$$

$$q_t = q_e - \left(q_e{}^{1-n} - \frac{k}{1-n}t\right)^{\frac{1}{1-n}} \quad \text{Ritchie model} \tag{4}$$

The results of adsorption kinetics are shown in Fig. 7. The fitting parameters of the four models are shown in Table 2. The correlation coefficient of the pseudo-second-order kinetics is higher than that of the pseudo-first-order order kinetics. In addition, the equilibrium adsorption amount obtained by fitting the pseudo-second-order kinetic model is consistent with the equilibrium adsorption amount obtained by experiments. This shows that the pseudo-second-order kinetic model can explain the adsorption mechanism of Cr(VI) by PM-biochar. Therefore, the adsorption process meets the assumption of second-order kinetics that the adsorption process is considered to be a chemical process.

Table 5
Thermodynamic parameters for Cr(VI) adsorption on biochar.

T (K)	K_d	ΔG^0 (kJ mol^{-1})	ΔH^0 (kJ mol^{-1})	ΔS^0 (J mol^{-1} K)
289.15	11.05	−6.17		
299.15	21.35	−7.36	30.527	126.82
309.15	33.2	−8.70		

3.6. Adsorption isotherms

Two isotherm models were adopted to simulate the adsorption of Cr (VI) from biochar.

$$q_e = \frac{Q_0 k_L C_e}{1+K_L C_e} \quad \text{Langmuir model} \tag{5}$$

$$q_e = K_f C_e{}^{1/n} \quad \text{Freundlich model} \tag{6}$$

As shown in Fig. 9, the adsorption amount increases with the increase of the initial Cr(VI) concentration. When the initial concentration of Cr(VI) in the aqueous solution is 500 mg L^{-1}, the adsorption amount is basically saturated, that is, the maximum saturated adsorption value is 157.9 mg g^{-1}. The relevant parameters of the two models are shown in Table 3. It shows that the correlation coefficient of the Langmuir model is larger than that of the Freundlich model for distillers grain biochar, which indicates that the adsorption of Cr(VI) by distillers grain biochar is more consistent with the Langmuir model, that is, Cr (VI) is adsorbed onto the surface of distillers grain biochar by uniform energy, mainly by monolayer adsorption. For PM-biochar, the Freundlich model better describes its adsorption process for Cr(VI), indicating that Cr(VI) adsorption to PM-biochar is attributed to its surface functional groups and calcium cations.

As shown in Table 4, compared with other related adsorbents, the PM-biochar prepared in this study has a relatively good adsorption effect on Cr(VI). Therefore, from the aspects of preparation cost, raw material source, and environmental benefit, PM-biochar could be as a promising adsorbent worthy of promotion in the treatment of chromium-containing wastewater.

3.7. Adsorption thermodynamics

The thermodynamics of Cr(VI) adsorption on the PM-biochar at 289.15 K, 299.15 K, and 309.15 K was analyzed, respectively. The thermodynamic equations can be written as follows:

$$\Delta G^0 = -RT\ \ln K_d \tag{7}$$

$$\Delta G^0 = \Delta H^0 - T\Delta S^0 \tag{8}$$

$$\ln K_d = \frac{\Delta S^0}{R} - \frac{\Delta H^0}{RT} \tag{9}$$

In the above equation, ΔG^0, ΔH^0, and ΔS^0 represent the Gibbs free energy change (kJ·mol^{-1}), enthalpy change (kJ·mol^{-1}) and entropy change of biochar on the isothermal adsorption process of Cr(VI), respectively (kJ·mol^{-1}); R is the ideal gas state equation constant 8.314 J·mol^{-1} K^{-1}; T is the thermodynamic temperature, K; K_d is the adsorption equilibrium constant (K) from the value of the best fit nonlinear isotherm equilibrium model (Lima et al., 2015), which is calculated using the method recommended by Lima et al. (2019).

Fig. 10 shows that as the ambient temperature increases, the maximum amount of adsorption also increases. At the initial concentration of the solution of 50 mg L^{-1} and three temperatures, the ΔG^0 of Cr (VI) is negative and gradually decreases with the increase of temperature. Therefore, the process of adsorbing Cr(VI) by PM-biochar is an endothermic process, which is consistent with other studies (Gan et al., 2015). The ΔH^0 and ΔS^0 are both positive (Table 5). The negative values of ΔG^0 from −6.17 to −8.70 kJ mol^{-1} indicate that the adsorption of Cr

(VI) onto PM-biochar is feasible and spontaneous, and a larger negative value indicates that the reaction proceeds more thoroughly and more Cr (VI) adsorbed with the increasing temperature. Entropy change (ΔS^0) is a positive value, which means that the order of the system is enhanced. In the system composed of biochar and Cr(VI), it is also indicated that biochar can adsorb Cr(VI) more firmly. The enthalpy change (ΔH^0) is positive, indicating that the Cr(VI) adsorption process is primarily endothermic and chemical in the PM-biochar and Cr(VI).

4. Conclusions

A new type of PM-biochar composite was prepared, which has an ideal adsorption potential for Cr(VI). The maximum Cr(VI) adsorption capacity reaches 157.9 mg g^{-1}. The adsorption process of Cr(VI) by PM-biochar is largely affected by solution pH. The Cr(VI) adsorption by PM-biochar conforms to the pseudo-second-order kinetic and Freundlich model, indicating that the adsorption is a chemical process. Thermodynamic studies show that the Cr(VI) adsorption by PM-biochar is a spontaneous endothermic process. Future studies are necessary to carry out in actual wastewater and contaminated soils.

Declaration of Competing Interest

The authors declare that they have no known competing financial interests or personal relationships that could have appeared to influence the work reported in this paper.

Acknowledgments

This work was supported by the National Key Research and Development Program of China (2016YFC0502602), the National Natural Science Foundation of China (U1612441), the High-Level Overseas Talent Innovation and Entrepreneurship Project of Guizhou Province (201808) and the Opening Fund of State Key Laboratory of Environmental Geochemistry (SKLEG2019704).

References

EPA, 1990. Environmental Pollution Control Alternatives: Drinking Water Treatment for Small Communities. Center for Environmental Research Information.
Ahmad, M., Rajapaksha, A.U., Lim, J.E., Zhang, M., Bolan, N., Mohan, D., Vithanage, M., Lee, S.S., Ok, Y.S., 2014. Biochar as a sorbent for contaminant management in soil and water: a review. Chemosphere 99, 19–33.
Aksu, Z., Gönen, F., Demircan, Z., 2002. Biosorption of chromium(VI) ions by Mowital®-B30H resin immobilized activated sludge in a packed bed: comparison with granular activated carbon. Process Biochem. 38, 175–186.
Altun, T., Kar, Y., 2016. Removal of Cr(VI) from aqueous solution by pyrolytic charcoals. New Carbon Mater. 31, 501–509.
ASTM, 2007. D1762-84 Standard Test Method for Chemical Analysis of Wood Charcoal. ASTM International, Conshohocken,PA.
Baral, A., Engelken, R.D., 2002. Chromium-based regulations and greening in metal finishing industries in the USA. Environ. Sci. Pol. 5, 121–133.
Chen, S.-S., Li, C.-W., Hsu, H.-D., Lee, P.-C., Chang, Y.-M., Yang, C.-H., 2009. Concentration and purification of chromate from electroplating wastewater by two-stage electrodialysis processes. J. Hazard. Mater. 161, 1075–1080.
Dehghani, M.H., Sanaei, D., Ali, I., Bhatnagar, A., 2016. Removal of chromium(VI) from aqueous solution using treated waste newspaper as a low-cost adsorbent: kinetic modeling and isotherm studies. J. Mol. Liq. 215, 671–679.
Dong, X., Ma, L.Q., Li, Y., 2011. Characteristics and mechanisms of hexavalent chromium removal by biochar from sugar beet tailing. J. Hazard. Mater. 190, 909–915.
Dong, H., Deng, J., Xie, Y., Zhang, C., Jiang, Z., Cheng, Y., Hou, K., Zeng, G., 2017. Stabilization of nanoscale zero-valent iron (nZVI) with modified biochar for Cr(VI) removal from aqueous solution. J. Hazard. Mater. 332, 79–86.
Gan, C., Liu, Y., Tan, X., Wang, S., Zeng, G., Zheng, B., Li, T., Jiang, Z., Liu, W., 2015. Effect of porous zinc–biochar nanocomposites on Cr (vi) adsorption from aqueous solution. RSC Adv. 5, 35107–35115.
Gheju, M., Balcu, I., 2011. Removal of chromium from Cr(VI) polluted wastewaters by reduction with scrap iron and subsequent precipitation of resulted cations. J. Hazard. Mater. 196, 131–138.
Han, Y., Cao, X., Ouyang, X., Sohi, S.P., Chen, J., 2016. Adsorption kinetics of magnetic biochar derived from peanut hull on removal of Cr (VI) from aqueous solution: effects of production conditions and particle size. Chemosphere 145, 336–341.
Hu, J., Chen, G., Lo, I.M.C., 2005. Removal and recovery of Cr(VI) from wastewater by maghemite nanoparticles. Water Res. 39, 4528–4536.
Huang, X., Liu, Y., Liu, S., Tan, X., Ding, Y., Zeng, G., Zhou, Y., Zhang, M., Wang, S., Zheng, B., 2016. Effective removal of Cr (VI) using β-cyclodextrin–chitosan modified biochars with adsorption/reduction bifuctional roles. RSC Adv. 6, 94–104.
Jiang, L., Liu, S., Liu, Y., Zeng, G., Guo, Y., Yin, Y., Cai, X., Zhou, L., Tan, X., Huang, X., 2017. Enhanced adsorption of hexavalent chromium by a biochar derived from ramie biomass (Boehmeria nivea (L.) Gaud.) modified with β-cyclodextrin/poly(L-glutamic acid). Environ. Sci. Pollut. Res. 24, 23528–23537.
Kim, S.D., Park, K.S., Gu, M.B., 2002. Toxicity of hexavalent chromium to Daphnia magna: influence of reduction reaction by ferrous iron. J. Hazard. Mater. 93, 155–164.
Kumar, R., Bishnoi, N.R., Garima Bishnoi, K., 2008. Biosorption of chromium(VI) from aqueous solution and electroplating wastewater using fungal biomass. Chem. Eng. J. 135, 202–208.
Kurniawan, T.A., Chan, G.Y.S., Lo, W.-H., Babel, S., 2006. Physico–chemical treatment techniques for wastewater laden with heavy metals. Chem. Eng. J. 118, 83–98.
Lim, A.P., Aris, A.Z., 2014. A review on economically adsorbents on heavy metals removal in water and wastewater. Rev. Environ. Sci. Biotechnol. 13, 163–181.
Lima, É.C., Adebayo, M.A., Machado, F.M., 2015. Kinetic and Equilibrium Models of Adsorption. Carbon Nanomaterials as Adsorbents for Environmental and Biological Applications. Springer, pp. 33–69.
Lima, E.C., Hosseini-Bandegharaei, A., Moreno-Piraján, J.C., Anastopoulos, I., 2019. A critical review of the estimation of the thermodynamic parameters on adsorption equilibria. Wrong use of equilibrium constant in the Van't Hoof equation for calculation of thermodynamic parameters of adsorption. J. Mol. Liq. 273, 425–434.
Liu, K., Rosentrater, K.A., 2016. Distillers Grains: Production, Properties, and Utilization. CRC Press.
López-García, M., Lodeiro, P., Barriada, J.L., Herrero, R., Sastre de Vicente, M.E., 2010. Reduction of Cr (VI) levels in solution using bracken fern biomass: batch and column studies. Chem. Eng. J. 165, 517–523.
Mao, N., Yang, L., Zhao, G., Li, X., Li, Y., 2012. Adsorption performance and mechanism of Cr (VI) using magnetic PS-EDTA resin from micro-polluted waters. Chem. Eng. J. 200-202, 480–490.
Miretzky, P., Cirelli, A.F., 2010. Cr(VI) and Cr(III) removal from aqueous solution by raw and modified lignocellulosic materials: a review. J. Hazard. Mater. 180, 1–19.
Mohan, D., Sarswat, A., Ok, Y.S., Pittman Jr., C.U., 2014. Organic and inorganic contaminants removal from water with biochar, a renewable, low cost and sustainable adsorbent – a critical review. Bioresour. Technol. 160, 191–202.
Namasivayam, C., Sureshkumar, M.V., 2008. Removal of chromium(VI) from water and wastewater using surfactant modified coconut coir pith as a biosorbent. Bioresour. Technol. 99, 2218–2225.
Ouyang, X., Han, Y., Cao, X., Chen, J., 2017. Magnetic biochar combining adsorption and separation recycle for removal of chromium in aqueous solution. Water Sci. Technol. 75, 1177–1184.
Owlad, M., Aroua, M.K., Daud, W.A.W., Baroutian, S., 2009. Removal of hexavalent chromium-contaminated water and wastewater: a review. Water Air Soil Pollut. 200, 59–77.
Pan, J.-j., Jiang, J., Xu, R.-k., 2014. Removal of Cr(VI) from aqueous solutions by Na_2SO_3/$FeSO_4$ combined with peanut straw biochar. Chemosphere. 101, 71–76.
Park, D., Lim, S.-R., Yun, Y.-S., Park, J.M., 2008. Development of a new Cr(VI)-biosorbent from agricultural biowaste. Bioresour. Technol. 99, 8810–8818.
Pellerin, C., Booker, S.M., 2000. Reflections on hexavalent chromium: health hazards of an industrial heavyweight. Environ. Health Perspect. 108, 402–407.
Pratush, A., Kumar, A., Hu, Z., 2018. Adverse effect of heavy metals (As, Pb, Hg, and Cr) on health and their bioremediation strategies: a review. Int. Microbiol. 21, 97–106.
Rajapaksha, A.U., Chen, S.S., Tsang, D.C., Zhang, M., Vithanage, M., Mandal, S., Gao, B., Bolan, N.S., Ok, Y.S., 2016. Engineered/designer biochar for contaminant removal/immobilization from soil and water: potential and implication of biochar modification. Chemosphere 148, 276–291.
Rajapaksha, A.U., Alam, M.S., Chen, N., Alessi, D.S., Igalavithana, A.D., Tsang, D.C.W., Ok, Y.S., 2018. Removal of hexavalent chromium in aqueous solutions using biochar: chemical and spectroscopic investigations. Sci. Total Environ. 625, 1567–1573.
Rangabhashiyam, S., Selvaraju, N., 2015. Adsorptive remediation of hexavalent chromium from synthetic wastewater by a natural and $ZnCl_2$ activated Sterculia guttata shell. J. Mol. Liq. 207, 39–49.
Rutherford, P.M., Dudas, M.J., Samek, R.A., 1994. Environmental impacts of phosphogypsum. Sci. Total Environ. 149, 1–38.
Saha, B., Orvig, C., 2010. Biosorbents for hexavalent chromium elimination from industrial and municipal effluents. Coord. Chem. Rev. 254, 2959–2972.
Sahu, J.N., Acharya, J., Meikap, B.C., 2009. Response surface modeling and optimization of chromium(VI) removal from aqueous solution using tamarind wood activated carbon in batch process. J. Hazard. Mater. 172, 818–825.
Shaheen, S.M., Niazi, N.K., Hassan, N.E.E., Bibi, I., Wang, H., Tsang Daniel, C.W., Ok, Y.S., Bolan, N., Rinklebe, J., 2019. Wood-based biochar for the removal of potentially toxic elements in water and wastewater: a critical review. Int. Mater. Rev. 64, 216–247.
Shang, M.R., Liu, Y.G., Liu, S.B., Zeng, G.M., Tan, X.F., Jiang, L.H., Huang, X.X., Ding, Y., Guo, Y.M., Wang, S.F., 2016. A novel graphene oxide coated biochar composite: synthesis, characterization and application for Cr (VI) removal. RSC Adv. 6, 85202–85212.
Shi, S., Yang, J., Liang, S., Li, M., Gan, Q., Xiao, K., Hu, J., 2018. Enhanced Cr(VI) removal from acidic solutions using biochar modified by Fe_3O_4@SiO_2-NH_2 particles. Sci. Total Environ. 628-629, 499–508.
Shu, Y., Tang, C., Hu, X., Jiang, L., Hu, X., Zhao, Y., 2018. H_3PO_4-activated cattail carbon production and application in chromium removal from aqueous solution: process optimization and removal mechanism. Water 10, 754.
Tong, X.-J., Li, J.-y., Yuan, J.-h., Xu, R.-K., 2011. Adsorption of Cu(II) by biochars generated from three crop straws. Chem. Eng. J. 172, 828–834.

Wang, B., Lehmann, J., Hanley, K., Hestrin, R., Enders, A., 2015. Adsorption and desorption of ammonium by maple wood biochar as a function of oxidation and pH. Chemosphere 138, 120–126.
Wang, B., Lehmann, J., Hanley, K., Hestrin, R., Enders, A., 2016. Ammonium retention by oxidized biochars produced at different pyrolysis temperatures and residence times. RSC Adv. 6, 41907–41913.
Wang, B., Gao, B., Fang, J., 2017. Recent advances in engineered biochar productions and applications. Crit. Rev. Environ. Sci. Technol. 47, 2158–2207.
Wang, B., Gao, B., Wan, Y., 2018. Entrapment of ball-milled biochar in Ca-alginate beads for the removal of aqueous Cd(II). J. Ind. Eng. Chem. 61, 161–168.
Wang, Q., Wang, B., Lee, X., Lehmann, J., Gao, B., 2018. Sorption and desorption of Pb(II) to biochar as affected by oxidation and pH. Sci. Total Environ. 634, 188–194.
Wang, S., Zhao, M., Zhou, M., Li, Y.C., Wang, J., Gao, B., Sato, S., Feng, K., Yin, W., Deshani Igalavithana, A., Oleszczuk, P., Wang, X., Ok, Y.S., 2019. Biochar-supported nZVI (nZVI/BC) for contaminant removal from soil and water: a critical review. J. Hazard. Mater. 373, 820–834.
Xiao, X., Chen, B., Chen, Z., Zhu, L., Schnoor, J.L., 2018. Insight into multiple and multilevel structures of biochars and their potential environmental applications: a critical review. Environ. Sci. Technol. 52, 5027–5047.
Yang, P., Guo, D., Chen, Z., Cui, B., Xiao, B., Liu, S., Hu, M., 2017. Removal of Cr (VI) from aqueous solution using magnetic biochar synthesized by a single step method. J. Dispers. Sci. Technol. 38, 1665–1674.
Yu, J., Jiang, C., Guan, Q., Ning, P., Gu, J., Chen, Q., Zhang, J., Miao, R., 2018. Enhanced removal of Cr(VI) from aqueous solution by supported ZnO nanoparticles on biochar derived from waste water hyacinth. Chemosphere 195, 632–640.
Zhang, J., Zheng, P., 2015. A preliminary investigation of the mechanism of hexavalent chromium removal by corn-bran residue and derived chars. RSC Adv. 5, 17768–17774.
Zhao, Q., Wang, Y., Cao, Y., Chen, A., Ren, M., Ge, Y., Yu, Z., Wan, S., Hu, A., Bo, Q., Ruan, L., Chen, H., Qin, S., Chen, W., Hu, C., Tao, F., Xu, D., Xu, J., Wen, L., Li, L., 2014. Potential health risks of heavy metals in cultivated topsoil and grain, including correlations with human primary liver, lung and gastric cancer, in Anhui province, eastern China. Sci. Total Environ. 470–471, 340–347.
Zhao, N., Zhao, C., Lv, Y., Zhang, W., Du, Y., Hao, Z., Zhang, J., 2017. Adsorption and coadsorption mechanisms of Cr(VI) and organic contaminants on H_3PO_4 treated biochar. Chemosphere 186, 422–429.
Zhao, N., Yin, Z., Liu, F., Zhang, M., Lv, Y., Hao, Z., Pan, G., Zhang, J., 2018. Environmentally persistent free radicals mediated removal of Cr(VI) from highly saline water by corn straw biochars. Bioresour. Technol. 260, 294–301.
Zhou, H., Chen, Y., 2010. Effect of acidic surface functional groups on Cr(VI) removal by activated carbon from aqueous solution. Rare Metals 29, 333–338.
Zhou, Y., Jin, Q., Zhu, T., Akama, Y., 2011. Adsorption of chromium (VI) from aqueous solutions by cellulose modified with β-CD and quaternary ammonium groups. J. Hazard. Mater. 187, 303–310.
Zhou, Z., Liu, Y.-g., Liu, S.-b., Liu, H.-y., Zeng, G.-m., Tan, X.-f., Yang, C.-p., Ding, y, Yan, Z.-l., Cai, X.-x., 2017. Sorption performance and mechanisms of arsenic(V) removal by magnetic gelatin-modified biochar. Chem. Eng. J. 314, 223–231.